Snow Cover and Snow Mass Intercomparisons of General Circulation Models and Remotely Sensed Datasets

JAMES FOSTER,* GLEN LISTON,* RANDY KOSTER,* RICHARD ESSERY,[†] HELGA BEHR,[#] LYDIA DUMENIL,[#]
DIANA VERSEGHY,[@] STARLY THOMPSON,[&] DAVID POLLARD,[&] AND JUDAH COHEN[**]

*NASA, Goddard Space Flight Center, Greenbelt, Maryland
[†]United Kingdom Meteorological Office, Hadley Climate Centre, Bracknell, England
[#]University of Hamburg, Meteorology Institute, Hamburg, Germany
[@]Canadian Climate Centre, Atmospheric Environment Service, Downsview, Ontario, Canada
[&]National Center for Atmospheric Research, Interdisciplinary Climate Systems, Boulder, Colorado
[**]NASA, Goddard Institute for Space Studies, New York, New York

(Manuscript received 8 September 1994, in final form 2 August 1995)

ABSTRACT

Confirmation of the ability of general circulation models (GCMs) to accurately represent snow cover and snow mass distributions is vital for climate studies. There must be a high degree of confidence that what is being predicted by the models is reliable, since realistic results cannot be assured unless they are tested against results from observed data or other available datasets. In this study, snow output from seven GCMs and passive-microwave snow data derived from the Nimbus-7 Scanning Multichannel Microwave Radiometer (SMMR) are intercompared. National Oceanic and Atmospheric Administration satellite data are used as the standard of reference for snow extent observations and the U.S. Air Force snow depth climatology is used as the standard for snow mass. The reliability of the SMMR snow data needs to be verified, as well, because currently this is the only available dataset that allows for yearly and monthly variations in snow depth. [The GCMs employed in this investigation are the United Kingdom Meteorological Office, Hadley Centre GCM, the Max Planck Institute for Meteorology/University of Hamburg (ECHAM) GCM, the Canadian Climate Centre GCM, the National Center for Atmospheric Research (GENESIS) GCM, the Goddard Institute for Space Studies GCM, the Goddard Laboratory for Atmospheres GCM and the Goddard Coupled Climate Dynamics Group (AIRES) GCM.] Data for both North America and Eurasia are examined in an effort to assess the magnitude of spatial and temporal variations that exist between the standards of reference, the models, and the passive microwave data. Results indicate that both the models and SMMR represent seasonal and year-to-year snow distributions fairly well. The passive microwave data and several of the models, however, consistently underestimate snow mass, but other models overestimate the mass of snow on the ground. The models do a better job simulating winter and summer snow conditions than in the transition months. In general, the underestimation by SMMR is caused by absorption of microwave energy by vegetation. For the GCMs, differences between observed snow conditions can be ascribed to inaccuracies in simulating surface air temperatures and precipitation fields, especially during the spring and fall.

1. Introduction

The performance of general circulation models (GCMs) in predicting snow fields needs to be tested to quantitatively study the effects of snow on climate. Simulations of atmospheric flow using GCMs have achieved a high level of quality; however, evaluation of model parameters such as snow has been hindered by the lack of quality large-scale data for thickness (Arpe et al. 1993). Regardless of how sophisticated GCMs are, they must be used with care and tested against results from observed data or other available datasets in order to assure realistic results. Only when there is a high degree of confidence that land surface datasets such as snow cover and snow depth are reliable can they be used to evaluate the performance of GCMs (Foster et al. 1994). Snow is a particularly good diagnostic for evaluation since in order to correctly model snow cover and snow thickness, both the temperature and precipitation schemes need to be realistic.

National Oceanic and Atmospheric Administration (NOAA) visible satellite data of snow permit direct observations of snow extent and afford direct comparisons with climatological and synoptic measurements. Because passive microwave satellite data require algorithms to derive snow extent and thickness, the estimates are not as direct as those from the visible data.

Corresponding author address: Dr. James Foster, Hydrological Sciences Branch, NASA Goddard Space Flight Center, Greenbelt, MD 20771.
E-mail: jfoster@glacier.gsfc.nasa.gov

Presently, the value of the microwave data is that it is the only snow depth dataset that varies from year to year. However, improvements in snow depth derivations must be made before the models can use the microwave data to confirm their simulations and eventually, perhaps, for initial conditions.

The purpose of this paper is to quantitatively determine how GCMs perform in terms of snow extent and snow storage at continental scales. The differences will be assessed by comparing model results from several GCMs with climatological data and remotely sensed data (visible data and passive microwave data). In addition, why discrepancies exist between the models and the climatological and remote sensing data will be addressed. It is important that these questions be answered to validate the model outputs. Quantifying the ability of GCMs to represent the global hydrologic cycle is an important component of the Atmospheric Modeling Intercomparison Project (AMIP), which is using a 10-yr period to intercompare model output from more than two dozen GCMs. The intent of this intercomparison is not to find the GCM that works best in all circumstances but rather to identify and redress possible deficiencies in the models. An additional objective is to evaluate the accuracy of the passive microwave estimates.

Because the models and the remotely sensed data used here have different resolutions, the snow measurement comparisons are based on slightly different land surface areas. If the goal of the study were solely to determine which model is best then it would make sense to interpolate all of the data onto the same grid. However, this cannot now be determined, since there is no way of knowing whether differences are a result of model error or observational inaccuracies. Also, because the datasets that are being used as "standards" are themselves likely to have some biases, a more rigorous numerical comparison between the observed and the modeled values is not presented in this paper.

Only in recent years have sophisticated modeling techniques been employed to look at the influence of snow cover globally. For example, Walsh and Ross (1988) used the National Center for Atmospheric Research (NCAR) Community Forecast Model (CFM) to see how snow and ice influence the synoptic features of the atmosphere. They showed that large snow cover extent results in lower geopotential heights and lower sea level pressures along eastern North America, and that near surface temperatures are colder locally when greater snow cover is prescribed in the model run. Barnett et al. (1987), using a version of the European Centre for Medium-Range Weather Forecasts (ECMWF) model, found that large-scale changes in Eurasian snow cover are coupled to larger-scale changes in the global climate system, and that snow cover effects alter climatic fields known to be intimately associated with the El Niño/Southern Oscillation (ENSO) phenomenon. A group of 38 scientists used 17 GCMs to assess whether

the presence of snow always produces a positive feedback (Cess et al. 1991). In most global warming scenarios, a warmer climate would melt more snow, thereby exposing darker surfaces that would make the earth even warmer. An intercomparison of the models suggests that this explanation is overly simplistic and demonstrates that snow feedback is associated with a multitude of complexities.

2. Datasets

A number of modeling groups have agreed to share their GCM data for this study. The Hadley Centre (HC model) in Bracknell, England; the Canadian Climate Centre (CCC model) in Downsview, Ontario; The National Center for Atmospheric Research (GENESIS model) in Boulder, Colorado; the Max Planck Institute for Meteorology (ECHAM model) in Hamburg, Germany; the Goddard Institute for Space Studies (GISS model), in New York; and the Goddard Space Flight Center (GLA and ARIES models) in Greenbelt, Maryland, have all provided snow mass and snow cover data. Most of the available GCMs formulate snow in a similar manner. Snow accumulation and melt are accounted for by applying energy balance and mass balance equations. Precipitation falls as snow when the temperature of the lowest atmospheric level is below 0°C (Cattle 1991). Snow thickness is calculated as a balance of snowfall, melting, and sublimation (Cess et al. 1991). However, differences in factors such as physical parameterizations, grid size, and albedo result in different values of snow extent and snow mass (Foster et al. 1994).

Snow mass, and not snow depth, is the modeled variable in each of the GCMs. This means that assumptions have to be made concerning snow density in order to connect depth to mass, which is also the case for both the SMMR and the SDC data. This can be a significant source of error in the comparisons between the various datasets.

How snow is treated in each of the models used in this study is described briefly below. The HC, ECHAM, GLA, CCC, and ARIES GCMs are all run during the AMIP period (1979–1988), whereas the GENESIS and GISS GCMs are run for nonspecified 10-yr and 5-yr periods, respectively. During the model simulations, sea ice extent and sea surface temperatures are prescribed and updated each month during the 10-yr period based on observations. Monthly average snow output in terms of snow cover and snow mass is generated for the 1979–1988 period. The AMIP period is concordant with the SMMR record (1978–1987), and thus intercomparison between the AMIP modeled snow results and the passive microwave snow estimates are of particular interest. The 5-yr and 10-yr model runs, not associated with the AMIP period, use prescribed sea ice and sea surface temperatures for initial conditions, but they use climatological sea ice and sea

surface temperatures for all other months of the model run period. Here CO_2 and the solar constant are held fixed during the AMIP runs. The GENESIS model predicts sea surface temperatures and sea ice conditions using a 50-m slab ocean and multilayer sea ice model.

a. The HC model

The HC GCM uses a four-layer soil model to calculate the surface temperature and the heat flux into the ground at each land point. The thermal influence of snow is represented by reducing the conductivity of the surface layer with increasing snow depth (a new snow model is being developed that represents the snowpack as a separate layer on top of the soil model). Energy input to the snowpack above that required to raise the temperature to 0°C is used to melt snow. In the presence of snow, roughness lengths are reduced from the characteristic values used for each type of model vegetation. Roughness lengths are limited to 0.5 mm for the deepest snows. The snow albedo is a function of snow depth, snow temperature, and vegetation type. To represent the aging of the snowpack, the albedo decreases as the snow temperature approaches the melting point. The resolution of this model is 2.5° lat × 3.75° long. See Gregory and Smith (1990) and Smith (1993) for more information.

b. The GENESIS model

With the NCAR GENESIS model (Version 1.02) [see Thompson and Pollard (1994) for more details] a standard multilayer scheme is used to represent snow cover both on land and on sea ice. The prognostic variables are the temperature of each layer and the total snow mass per unit horizontal area, although for convenience the latter is expressed in terms of fractional areal coverage and total snow thickness, as explained in the following paragraphs.

Heat diffuses linearly with temperature between the snow layers and between the bottom snow layer and the topmost soil layer. If the temperature of any snow layer becomes greater than the melting point, it is immediately reset to the melting point, some snow is melted to conserve heat, and the meltwater is passed as water input to the soil model. Percolation and refreezing within the snowpack are neglected.

A minimum total snow thickness of 15 cm is imposed, so that when snowfall begins at a previously snow-free grid point, the fractional coverage increases from zero with snow thickness fixed at 15 cm. If the snowfall continues, the fractional coverage increases to a maximum of 100%, after which the thickness increases with fractional cover fixed at 100%. The reverse sequence occurs when a thick snow cover melts away. The snow is considered to bury bare ground and the lower vegetation alike with the same fractional coverage, ignoring any effects of the lower-story height.

To crudely account for the lower albedo of wet snow, the snow albedo depends on the topmost layer temperature. Below −15°C the visible and near-infrared albedos are 0.9 and 0.6, respectively, and decrease linearly to 0.7 and 0.4 as the temperature increases to 0°C (Harvey 1988). For the direct beam, the model uses the same dependence on solar zenith angle as in Briegleb and Ramanathan (1982). The effects of snow aging are ignored. This GCM has a resolution of 4.5° lat × 7.5° long.

c. The ECHAM model

The ECHAM GCM has evolved in several stages from a straightforward application of a low-resolution version of the ECMWF operational forecast model (Fischer 1987) to the present model, which was released in August 1990 (Roeckner et al. 1992). AMIP integrations cover the period from 1979 to 1988, using a seasonal cycle of solar radiation, and are forced by observational sea surface temperatures. The ECHAM model is run for 20 years with the first year of the AMIP run being year 11.

Precipitation is computed separately for deep convection and large-scale stratiform condensation. For convective events, snowfall occurs if the surface temperature is below 0°C and the temperature of the first model level below 300 m is below −3°C. Stratiform precipitation occurs as snow if the temperature at its level of origin is below 0°C. All snow may melt on its way to the surface if the temperature in a model layer exceeds +2°C. Snow may accumulate in a single layer at the surface. This snowpack evolves according to the budget equation of the water equivalent of snow.

If the snow layer reaches the threshold of 0.025 m, a distinction is made between the soil (characteristics of loam) and the snow pack on top of it. The snow temperature may not exceed 0°C and snow melt is initiated if both the snowpack and the uppermost soil layer reach 0°C (Behr and Dumenil 1992).

The albedo of snow over land is computed from a background albedo (Geleyn and PreuB 1983), which is modified under certain temperature conditions (Robock 1980) and in the presence of forests (Roeckner et al. 1992). In addition, the location of forested areas are specified according to the dataset by Matthews (1983). The resolution of this model is 2.8° lat × 2.8° long.

d. The CCC model

The version of the CCC GCM used for the AMIP runs is GCMII. Treatment of snow in this model is very simple, and was reviewed in Verseghy (1991) and Verseghy (1992). The fractional snow cover of each grid cell reaches 1 when the snow mass equals 100 kg m^{-2}, and varies as the square root of the mass below that value. Heat capacity of the snow-covered ground is cal-

culated as the weighted average of an assumed effective snow heat capacity and the heat capacity of the underlying soil. The calculated heat of melting is partitioned likewise between the snow and the ground according to the fractional snow cover. Snow albedo varies with time according to a simple aging factor. The effective surface albedo is calculated by modifying the snow albedo according to a snow-masking depth, which varies with the height of the vegetation present on the grid cell. A grid size of 3.75° lat × 3.75° long is used for this model.

e. The GLA model

This version of the Goddard Laboratory for Atmospheres (GLA) GCM uses the Xue et al. (1991) simplification of the Simple Biosphere Model (SiB) of Sellers et al. (1986). In the model, the effects of snow and ice have been accounted for by modifying some of the relevant SiB parameters and calculations.

Precipitation is assumed to fall as snow if the air temperature at a reference height is lower than the water freezing point. This snowfall is able to accumulate on the vegetation until some maximum holding capacity is reached, at which time the snow accumulates on the ground. The snow depth on the ground is computed assuming a snow density of 200 kg m^{-3}. The turbulent transfer coefficients are adjusted to account for the burying of vegetation by the snow.

The fractional area of the ground covered by snow varies linearly as a function of snow depth, reaching complete coverage when the snow volume corresponds to a snow depth of 0.05 m. The albedo of the snow-covered ground is determined from an area-fraction weighting of the snow albedo and the albedo of the snow-free ground. The snow albedo is assumed to be 0.8 in the visible and 0.4 in the near-infrared wavelength intervals. To account for melting conditions, these albedos are reduced by 60% when the surface temperature is at or near the melting temperature.

In the presence of snow, the surface temperature is not allowed to rise above the melting temperature. Any excess energy that would be available to raise the surface temperature above that of melting is applied toward melting the snow cover. Runoff from snowmelt can occur when the ground temperature is at, or near, the melting temperature (within 0.5°C). When the ground temperature is less than this near-melting temperature, neither infiltration nor runoff occurs. This model has a resolution of 4° lat × 5° long.

f. The ARIES model

The ARIES GCM, designed at NASA/GSFC for studies of natural (decadal) climate variability, is currently coupled to a land surface model that includes explicit vegetation control over the surface energy balance (Koster and Suarez 1992), and it is sometimes coupled to a full ocean model for studies of variability within the land/atmosphere/ocean system. The model's behavior, and particularly the land/atmosphere coupling, is documented by Koster and Suarez (1994).

Treatment of snow in the model is not especially sophisticated but does satisfy all water and energy balance constraints. Precipitation is deposited as snow when the surface air temperature lies below 0°C. Snow depth is a prognostic variable; deposited snow remains on the surface until it sublimates or melts away. The energy required for sublimation or melting can be extracted from the net radiation or the deep soil. The land surface remains at 0°C while the snow melts.

Snow affects the energy balance mostly through its high albedo, currently taken to be 0.85 for visible wavelengths and 0.5 for near-infrared wavelengths, regardless of snow age or assumed density. The model accounts for fractional areal coverage of snow; following the formulation in BATS (Dickinson et al. 1986), the fractional area A_f covered by snow having a domain-averaged depth of S (water equivalent) is taken to be $A_f = S/(S + So)$, where So is a constant for each vegetation type. The presence of snow does not modify roughness lengths. A resolution of 4° lat × 5° long is used for this model.

g. The GISS model

The GISS general circulation model is described in full by Hansen et al. (1983). In the GISS model, precipitation can occur from two physical processes, large-scale stratiform condensation and condensation caused by convection. In the model, precipitation will fall as snow if the lowest layer air temperature is less than 0°C. Snow can accumulate on land, land ice, or sea ice. The snow will accumulate if the upper layer ground temperature is less than or equal to 0°C. If the ground temperature is above 0°C, then the snow will melt, and the extraction of latent heat will lower the ground temperature. Heating of a snow covered surface will raise the ground temperature as high as 0°C, after which additional heating melts the snow. Only once all the snow has melted can the surface temperature go above 0°C.

Snow on the ground affects the albedo of the ground, energy transfers between the ground and the atmosphere, and energy transfers within the ground. In the model, the calculated density of snow is 100 kg m^{-3}. The albedo of a snow-covered surface depends on snow depth, snow age, masking depth of the existing vegetation and the albedo of the underlying surface. In calculating the energy budgets of the ground surface, the model uses two ground layers. There is a single prognostic variable for temperature used for the dry earth and any snow cover that exists on the ground. Surface energy budgets are computed using this single temperature variable. Heat transfers between the first ground layer and the lowest layer of the atmosphere are dependent on the heat capacity of the first ground layer,

which is a function of snow mass. The heat capacity of the first ground layer includes a mass-weighted fraction of snow multiplied by the heat capacity for snow and ice and added to the total mass (water and dry earth) times its heat capacity. Thermal conductivity between ground layers one and two is a function of the snow mass in layer one. The resolution of the GISS GCM is 8° lat × 10° long.

h. Passive microwave data

Since November 1978, the SMMR instrument on the *Nimbus-7* satellite and the Special Sensor Microwave Imager (SSMI) on the Defense Meteorological Satellite Program (DMSP) satellites have been acquiring passive microwave data that can be used to estimate snow extent and snow depth. The algorithm developed by Chang et al. (1987) uses the difference between the SMMR 37-GHz and 18-GHz channels to derive a snow depth/brightness temperature relationship for a uniform snow field. This is expressed as follows:

$$SD = 1.59(T_B18H - T_B37H),$$

where SD is snow depth in cm, T_B is the microwave brightness temperature, which is proportional to the surface emissivity and the physical temperature, H is the horizontal polarization, and 1.59 is a constant derived by using the linear portion of the 37- and 18-GHz responses to obtain a linear fit of the difference between the 18-GHz and 37-GHz frequencies. If the 18-GHz T_B is less than the 37-GHz T_B, the snow depth is defined to be zero. The snowpack density is assumed to be 300 kg m^{-3} and the average snow grain size within the snowpack is assumed to be 0.3 mm. This algorithm has a resolution of 0.5° lat × 0.5° long.

i. NOAA visible data

Since 1966, NOAA has prepared a weekly snow and ice boundary chart for the Northern Hemisphere. Monthly mean snow cover charts have been constructed from the weekly charts by deriving a subjective average of the weekly chart boundaries of each month. The areal extent of continental snow cover within this average monthly snow cover boundary is then measured and recorded. Each chart is the latest cloud-free snow observation, from the NOAA satellite imagery, of that particular area of the world. Monthly snow cover values are given for North America and Eurasia, as well as for the entire Northern Hemisphere (Matson and Wiesnet 1981; Matson et al. 1986).

The NOAA dataset is subject to inaccuracies in locating snowlines caused by prolonged periods of cloudiness in some areas and by analyst error in interpreting snow-free versus snow-covered terrain. However, the NOAA data are judged to be the most reliable of the available snow cover datasets.

j. Snow depth climatology (SDC)

The U.S. Air Force Environmental Technical Applications Center (USAF/ETAC) at Scott Air Force Base in Illinois has assembled a global snow depth climatology that is fully documented and is capable of being updated (Foster and Davy 1988). This global snow depth climatology uses a mesh reference grid that divides each hemisphere into 64 equal boxes. Each box is divided into 4096 grid points that are about 46 km apart. For each month, every box, and every grid point, a snow depth value (taken to be representative of the middle of the month) is assigned based on results primarily from climatological records, literature searches, surface-weather synoptic reports, and data obtained at snow course sites. The density used to convert snow depth to mass is 300 kg m^{-3}.

As with the NOAA data, this dataset is not without sources of error. In a number of countries, summarized snow depth values are not always available to construct a snow climatology with even a fair degree of confidence. Nevertheless, because in many cases the snow depths have been directly observed, these data are deemed to be the most reliable of the limited snow depth datasets available.

3. Study area

For the purposes of this study, North America encompasses all land areas between 10°W and 170°W longitude or between Newfoundland and Alaska. However, ice sheets are not counted in the snow cover calculations, since the emphasis in this study is seasonal snow only. Thus Greenland is excluded. Eurasia includes the areas between 170°W and 10°W longitude or between far-eastern Siberia and Great Britain.

4. Results

NOAA visible data were used as the standard to compare the modeled snow extent output and the passive microwave estimates. For snow mass measurements, the U.S. Air Force (USAF) snow depth climatology was used as the base line to compare modeled snow mass and microwave-derived estimates of snow mass. Snow mass is the derived snow depth times a specified density, and is given in units of 10^{13} kg. Snow extent is given in units of 10^6 km^2. Snow extent is the area covered by a thickness of at least 1 mm of snow water equivalent for the model data and at least 1-cm snow depth for the NOAA data.

A more rigid comparison might be between what the models, the SMMR data and the observations assume to constitute a complete snow cover. This varies from one data set to another. For instance, the CCC GCM assumes a complete cover when the snow mass reaches 10 kg m^{-2}. As previously mentioned, though, our interest is not to say definitively which of the models performs best, but rather to evaluate where and why
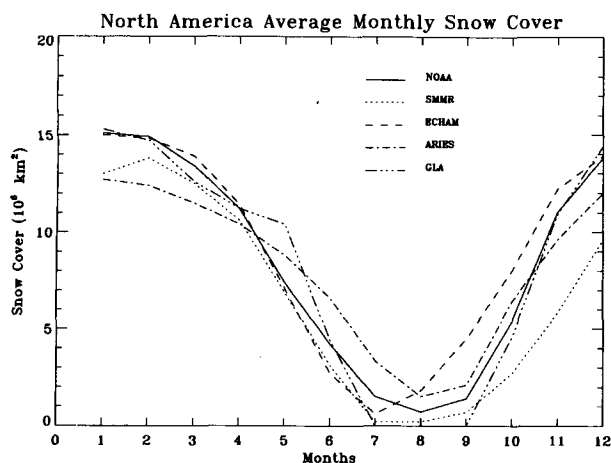
FIG. 1. Snow cover intercomparison for North America of results from NOAA, SMMR, and the ECHAM, ARIES, and GLA GCMs.
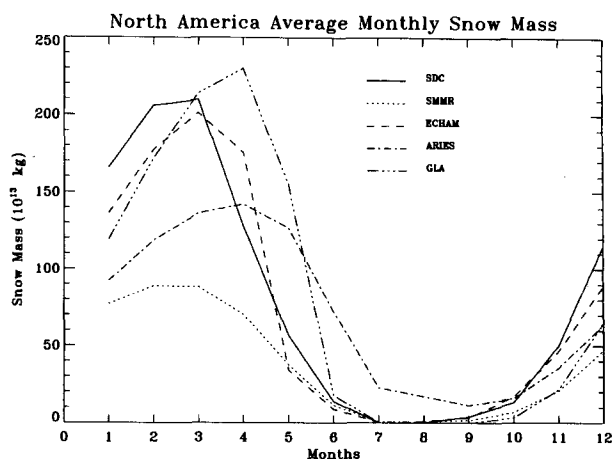

FIG. 3. Snow mass intercomparison for North America of results from a snow depth climatology, SMMR, and the ECHAM, ARIES, and GLA GCMs.

there is disagreement between the models, SMMR, and the observations.

Figures 1–8 show comparisons of the observed data (standards of reference) with the model results and SMMR estimates. These figures provide a measure of how well or poorly these different datasets agree with each other. Monthly NOAA and SMMR data were averaged for the period 1979–1987, and the monthly model results were averaged for the number of years they were run (either 5 or 10 yr). The interpretation of these figures will be discussed in section 5.

a. Significance tests

Significance tests were performed, using the t statistic test, to determine if differences between the modeled data and the observations were sufficiently small that they could be attributed to chance. For snow cover,

the monthly means of 10 years of NOAA data (1979–1988) were used to test significance levels.

For snow mass, the SDC data could not be used to test for significance, because the time period of measurement does not correspond with the AMIP period. To do a thorough validation, it is essential to know whether or not the differences between the datasets are statistically significant. Because the passive microwave dataset is the only snow mass dataset that permits month-to-month, as well as year-to-year, variability to be assessed, it is the only one that can be used to test for significance. Of course, the accuracy of this data must be systematically checked to ensure it is dependable enough for this purpose. For now, only snow cover can be tested for significance.

Differences between the SMMR and most of the modeled snow cover results were significant at the .05
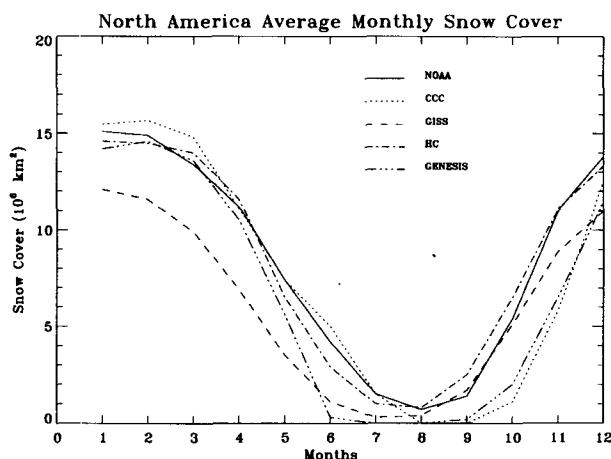

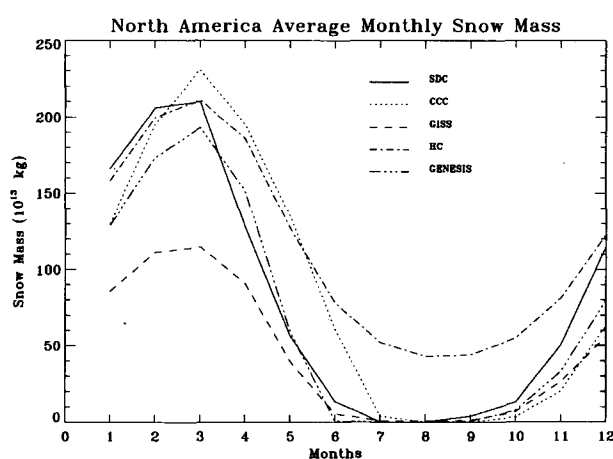FIG. 2. Same as Fig. 1 except for the HC, CCC, GISS, and GENESIS GCMs.

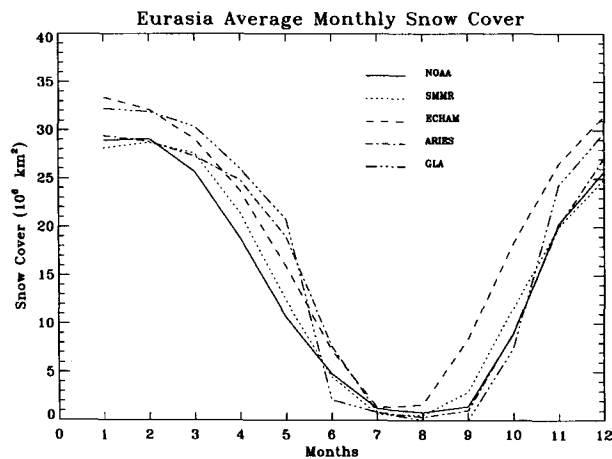FIG. 4. Same as Fig. 3 except for the HC, CCC, GISS, and GENESIS GCMs.

FIG. 5. Snow cover intercomparison for Eurasia of results from NOAA, SMMR, and the ECHAM, ARIES, and GLA GCMs.
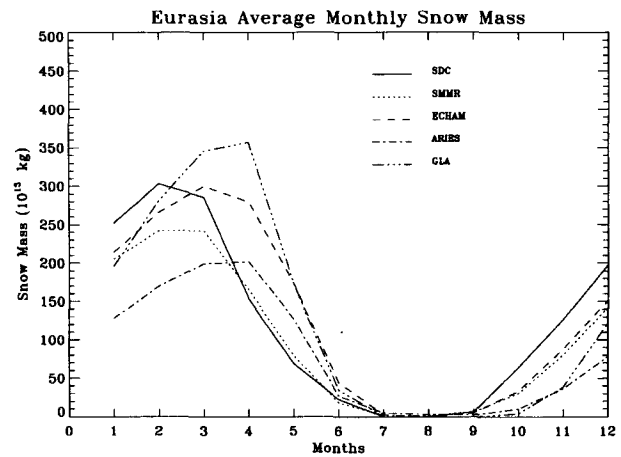

FIG. 7. Snow mass intercomparison for Eurasia of results from a snow depth climatology, SMMR, and the ECHAM, ARIES, and GLA GCMs.

level for nearly every month. However, the results of some models were significant in only certain seasons. For instance, in North America, the ECHAM model was significant in the winter months (January, February, and March), but not in September or October, and the ARIES model was significantly different in the autumn months (October, November, and December), but not in January or February.

b. Geographic snow cover and snow depth intercomparison for North America

Figures 9–18 show seasonal examples of modeled snow fields, climatological snow data, and remotely sensed NOAA and SMMR observations of snow for North America and Eurasia during the month of February. The intent in this section is to look at the seasonal distribution of snow on landmasses, for it is as impor-

tant to validate where areas of agreement and disagreement exist as it is to know the magnitude of the differences. Patterns of snow buildup and depletion are examined for average monthly data (mid-month except where otherwise noted). Although the figures only depict the February snow regime, snow conditions are described for May, July, and November, as well. For the NOAA data, snow cover frequency maps were used to assess the average snowline position (Matson et al. 1986).

For North American snow cover in February, the NOAA maps show the snow boundary very near the 40° latitude parallel (Fig. 9). This is true of most of the other datasets and models as well, although the CCC model locates the snow boundary too far south, and the GLA model shows excess snow in the southern plains of the United States. In eastern North America,
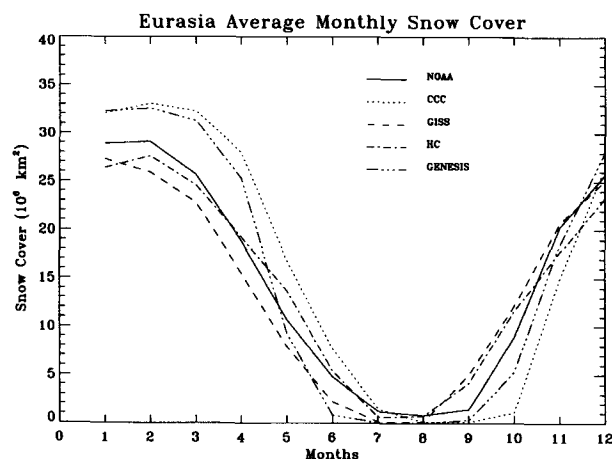

FIG. 6. Same as Fig. 5 except for the HC, CCC, GISS, and GENESIS GCMs.
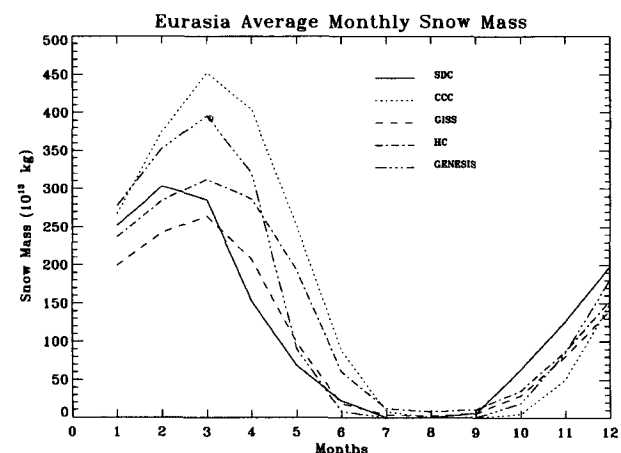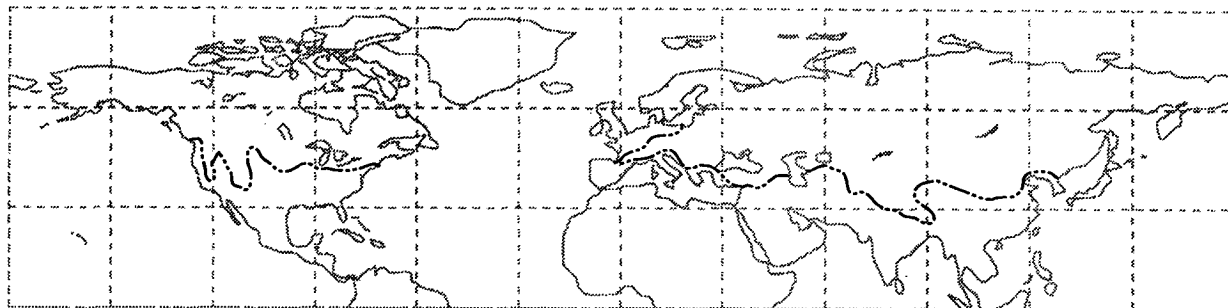

FIG. 8. Same as Fig. 7 except for the HC, CCC, GISS, and GENESIS GCMs.

NOAA Mean February Snow Cover

Contour at 1 cm snow depth

FIG. 9. Mean snow cover in the Northern Hemisphere from NOAA during February.

the SMMR snowline is located farther north than the NOAA and modeled snow fields.

The observed snowpack attains its' maximum thickness in February and March. The SDC map shows that there is a 75-cm contour (blackened area) southeast of Hudson Bay and north of Lake Superior. The SDC map, SMMR map, and the modeled snow fields all show a tongue of relatively shallow snow (less than 25 cm) extending from the U.S. Great Plains into the Canadian prairies. The modeled and remotely sensed snowpacks show comparable areas of buildup with the SDC maps; however, the magnitude of the buildup is noticeably smaller. On the SMMR map, the deepest snow is found in Alaska, the Yukon, and Northwest Territories, and east of Hudson Bay. Southeastern Canada, northeastern United States, and the Great Lakes regions are areas having too little snow. With the ECHAM data, the deepest snow is found in northeastern Canada and Alaska. The GLA model shows the most snow also in southeastern Canada, excluding mountainous snowpacks, but again the snow here, (about 50 cm) is less than that measured from the SDC data. The same is true with the HC snow fields, though in addition, the HC model shows deep snow south of Hudson Bay and in north central Canada.

By May the snow has retreated into central Canada. Despite deeper snowpacks in the spring, the snowline migrates faster than in the fall because of rapidly increasing solar insolation. According to the NOAA map for mid-May, the snow tends in a NW to SE direction from the Yukon Territory to Quebec. The shallower snow in interior areas has melted, so that the snow is generally positioned near the 60° latitude parallel west of Hudson Bay. To the east of Hudson Bay, some snow remains as far south as 50°. This is also the case with the SDC and SMMR maps, and with the HC-generated snow fields. With the ECHAM model, snow remains in the areas near the Mackenzie River Delta in far-northwestern Canada. The GLA model shows an ex-

cess of snow cover in southern Quebec and north of the Great Lakes.

At this time, the deepest snows (about 30 cm) are found northwest of Hudson Bay, according to the SDC data. The SMMR data reveal a similar pattern with 30 cm still on the ground in parts of Alaska, the Yukon Territory, and Labrador, as well. In between these areas the snowpack is shallow (<6 cm). The ECHAM model shows more than 50 cm of snow northwest of Hudson Bay and in Labrador. This is also true with the HC model. Although the GLA model snow fields again show a snow maximum northwest of Hudson Bay, in the Yukon Territory, and in Alaska, the most obvious feature is the excess of snow depth east of Hudson Bay where the snowpack has accumulated to 75 cm in thickness.

Only vestiges of the original snowpack remain by July, and there is no identifiable snowline. Most of the remaining (lowland) snow is located in the Canadian Archipelago north of the 70° parallel. Snow mass is negligible at this time of year. In fact, the SDC data indicate zero mass for both July and August. However, the HC model shows an excess of 59×10^{13} kg snow mass for the month of July in North America (about 30% of the February snow mass), even though the snow extent is comparable to the other models. Apparently all of the mass is being stored in mountainous high-latitude snowpacks.

In November, the average continental snowline on the NOAA snow map, on the SDC map, and on most of the model snow maps is positioned near the mouth of the St. Lawrence River in eastern Canada, just to the north of the Great Lakes, south of Lake Winnipeg, and close to the center of Alberta in western Canada. With the CCC model, the snowline is too far south at this time of year, and with the GENESIS model, the snowline is somewhat north of the actual or mapped location. The SMMR snowline is considerably north of the NOAA snowline, positioned adjacent to the center

SDC Mean February Snow Depth
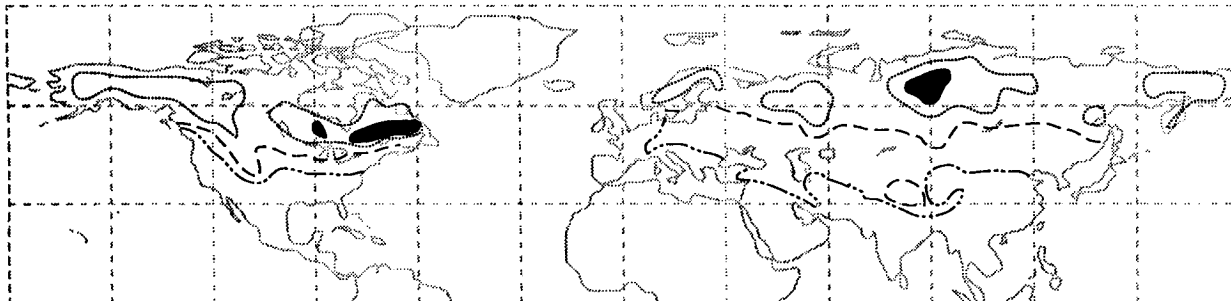
Contour at 2, 25, 50 and 75 cm snow depth

2cm = ·· — ·· , 25 cm = — — — , 50cm = · · · · , 75 cm = solid black

note — these lines are the same on each of the following maps

FIG. 10. Snow depth climatology map showing snow distribution in the Northern Hemisphere during February.

of Hudson Bay and in the vicinity of Great Slave Lake.

On the SDC map for November, the greatest snow depths (of about 25 cm) are located in Alaska, in the Yukon, and to the south and east of Hudson Bay. The SMMR snow maps also show the most snow in Alaska and Yukon, but no snow is shown south of Hudson Bay on the microwave maps. Snow thicknesses from the ECHAM data do not show areas that favor deeper snow, but this is probably a result of the contour internal (25 cm) being too large to discern November snow amounts. The HC and GLA models reasonably portray snow depth; however, in both cases, more snow is shown in northern Canada than exists according to the SDC data.

c. Geographic snow cover and snow depth intercomparison for Eurasia

As is the case in North America, in February, the NOAA snow boundary meanders about the 40° parallel (Fig. 9). In central Asia (the Tibet Plateau, the Himalayas, and the Caucasus) the snow cover protrudes well south of this parallel, and in western Europe, the snowline is closer to the 50° parallel. The SDC data shows this same pattern, as does the SMMR data. The snowline for the ARIES and the HC models is in most places slightly to the north of the NOAA snow boundary. In China, the ECHAM, GLA, and GENESIS models produce snow too far to the south of the NOAA-mapped boundary. The GISS model produces too little snow in the Steppes of Russia and Ukraine. Refer to Figs. 9–18.

The snow depths from the SDC maps show 50-cm depths in Scandinavia, the northern Urals (in northwestern Russia), and far eastern Siberia. In north-cen-

tral Siberia, the deepest nonmountainous snowpacks are found with depths of up to 75 cm. The ARIES model has a similar snow distribution as that of the SDC data. For SMMR, depths of over 50 cm occur in eastern and central Siberia, but in no area do depths of 75 cm occur. With the ECHAM data, too little snow is shown in east central Siberia. The HC-modeled snow fields have the snow distributed farther to the west than do the other datasets. The deepest snows (> than 75 cm) occur in Scandinavia and in northwestern Russia. With the CCC and GENESIS models, the greater snow mass results primarily from the deeper Himalayan snows and the excess snow cover produced in these models. The GISS-modeled snow fields show the deepest snows (> than 75 cm) in north-central and northeastern Siberia.

The snow boundary has retired to near the 60° parallel by mid-May, according to the NOAA snow map. The snowline is several hundred km to the south of this latitude in eastern Siberia, and several hundred km to the north of this latitude in western Russia. The SDC follows the NOAA snow boundary across western Russia; however, in eastern Siberia the SDC boundary is located closer to the 65° parallel. The SMMR snow boundary in eastern Siberia approximates the snowline from the NOAA maps. In western Russia, though, the SMMR snowline is too far to the north. In contrast, too much snow occurs on the Tibet Plateau. The ECHAM model snowline compares well with the NOAA snow boundary in western Russia, but in Siberia it is located somewhat south of the NOAA boundary. Again, with this model, there is an excess of snow on the Tibet Plateau. The HC, GLA, and CCC models generate too great a snow cover in all regions, but the ARIES model generates too little snow.

SMMR Mean February Snow Depth
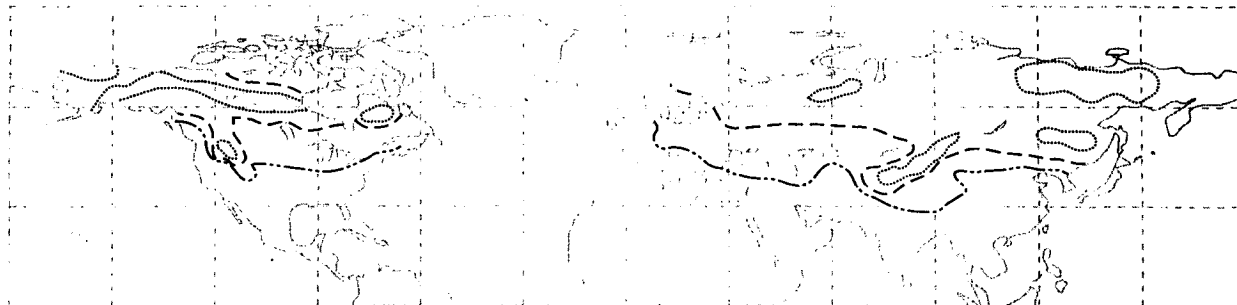
Contour at 2, 25, and 50 cm snow depth

FIG. 11. Same as Fig. 10 except from SMMR.

There are two primary foci of deep snow on the SDC snow maps for May. One area is located in extreme eastern Siberia and the other is in north-central Siberia. Both of these areas have depths of about 40 cm. In northern Scandinavia and in the northern Urals, the maximum thicknesses are about 30 cm. Snow depths from SMMR and from each of the models, except for ARIES, are greater than that from the SDC data. For SMMR, the pattern is unchanged from February, with the deepest snowpack (> 50 cm) found in north-central Siberia. Relatively deep snow still exists in Scandinavia and eastern Siberia (about 40 cm).

In midsummer (July), only a remnant of seasonal snow can be found along the Arctic coast in central and far eastern Siberia. The remotely sensed data and all of the models are consistent with this assessment except for the HC model and the CCC model. These two models produce too much snow cover in portions of the high Arctic, and hence the snow mass is also excessive, even though the depths are shallow (< 25 cm).

The NOAA data for Eurasia shows that by November, the snow cover has expanded south into Mongolia to the east and into the Steppe areas to the west. For the SDC and SMMR data, the snowline is in a similar position. The ECHAM model shows too much snow cover in central China, and the CCC and GLA models also show the snow boundary to be located too far to the south. However, the HC model shows too little snow with the location of the snowline close to the 50° parallel.

In regard to snow depth distribution, the SDC data shows that the deepest snows are found across central and eastern Siberia with a maximum of about 40 cm north of the 60° parallel in central Siberia. SMMR also shows a maximum snow thickness in these areas of about 40 cm. The ECHAM snow fields show a 50-cm contour around small areas of eastern and central Siberia. Snow depths produced by the HC model do not show regional maximums, but snowfields are typically deeper north of the 60° parallel.

5. Discussion

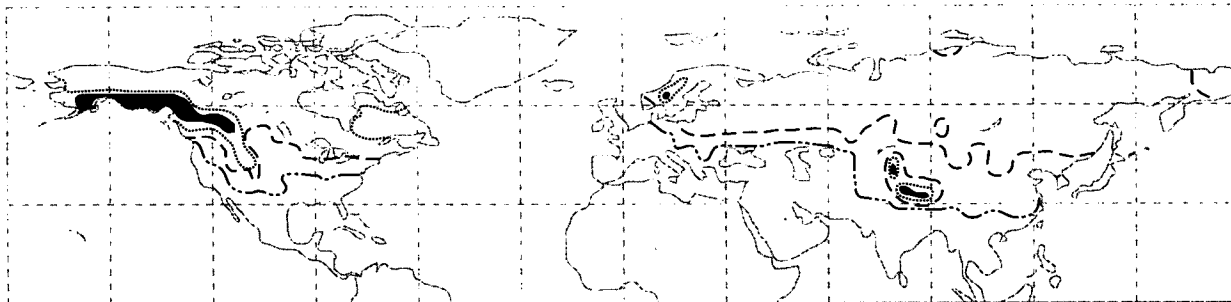As stated previously, the purpose of this intercomparison is to give modelers the opportunity to examine

HC Mean February Snow Depth
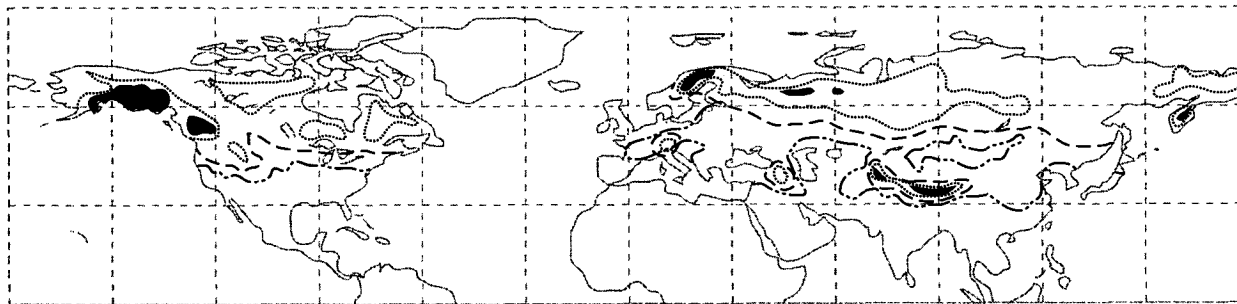
Contour at 2, 25, 50 and 75 cm snow depth

FIG. 12. Same as Fig. 10 except from the HC GCM.

GLA Mean February Snow Depth

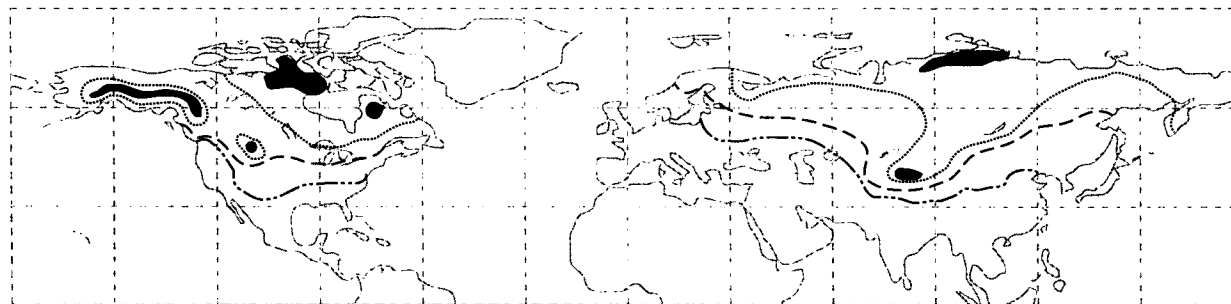## Contour at 2, 25, 50 and 75 cm snow depth

FIG. 13. Same as Fig. 10 except from the GLA GCM.

how several GCMs perform in terms of snow extent and snow mass when compared with observations. Since seasonal snow plays an important role in influencing the global radiation balance, the distribution and duration of snow needs to be well known in order for GCMs to portray the earth's climate in a faithful way. During the past decade, simulations of the atmospheric flow with GCMs have achieved a high degree of sophistication. Model verification, especially for snow depth, has been hindered by a lack of high-quality observational data. Because of limitations with the standards of reference used here, a certain amount of difference ascribed to errors in the models is actually due to deficiencies in the NOAA data and the SDC data. In terms of the SDC data, these deficiencies may be quite serious. For example, the dearth of meteorological stations in high mountainous areas generally results in an underestimation of the snowpack thickness in areas such as the Himalayan Ranges and the Rocky Mountains. Additionally, in many Arctic and even sub-Arctic locations, there are few reporting stations, and therefore

snow depth values must be interpolated by subjectively contouring the available point data. So, if the modelers attempt to improve their models using the SDC data, systematic errors may be inadvertently introduced (Groisman et al. 1993).

Another source of error that should not be overlooked results from constraints in the prescribed snow density imposed upon the SMMR and SDC datasets. Density is not a consideration in the interpretation of the GCMs since snow mass is a prognostic variable. The density of the snow is assumed to be 300 kg m^{-3} for both the SMMR and SDC data. Newly fallen snow may have a density that is closer to 100 kg m^{-3}, whereas aging snow in a ripe snowpack may have a density of 500 kg m^{-3}. The 300 kg m^{-3} value is what might be measured in snowpacks during the months of January, February, and March in much of the Northern Hemisphere. Higher densities would typically occur in April and May, while lower densities would be the rule during the autumn season. However, since the agreement between the SDC data and the SMMR data is
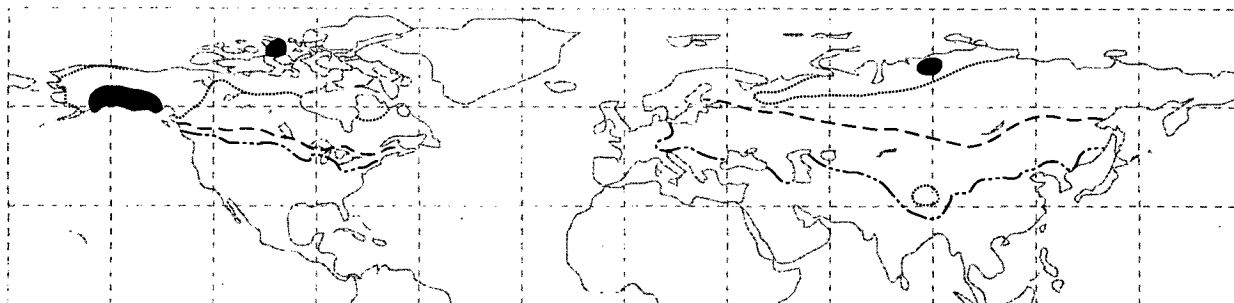
CCC Mean February Snow Depth

Contour at 2, 25, 50 and 75 cm snow depth

FIG. 14. Same as Fig. 10 except from the CCC GCM.

ARIES Mean February Snow Depth

Contour at 2, 25, 50 and 75 cm snow depth

FIG. 15. Same as Fig. 10 except from the ARIES GCM.

better in spring than in winter, increasing the SMMR springtime snow density would not improve the discrepancy in winter season snow mass. Because most of the models tend to overestimate snow mass in the spring, increasing the springtime density assumed for the SDC data would reduce the differences between the observations and the models.

Differences in snow extent during the late fall and early spring between the NOAA, microwave, and model datasets may be caused by the positioning of the snowline in the boreal forests. The visible sensors onboard the NOAA satellites are unable to penetrate dense forest covers and to monitor the underlying snow.

While most of the disagreement between the models and the NOAA and the SDC datasets seems to be related to inadequacies in the models' dynamics or physics packages, some of the differences can be explained by problems associated with grid scales and snow depth thresholds. For instance, not all of the models use the same size grid box. This may lead to an overestimation of snow extent and thus inflate snow mass values. Also,

most of the models use a contour level of 1 mm (about .3 or .4 cm depending upon the density) of snow water equivalent to define the snowline. With the NOAA data, the snowline, based on visible (.5–.7 μm) observations, is probably closer to a depth of about 2 cm of snow. Again, these differences will have a slight effect on continental snow extent and snow mass.

All of the models have difficulty in reliably portraying snow cover conditions in October. This is the month when snow cover first advances southward, and it appears that the models have a problem in gauging when snow expansion should begin.

Determining the source of problems or shortcomings or knowing what the differences between the models and the reference standards are attributed to is in some cases, a difficult proposition. Moreover, fixing the problems, once they have been identified, is not so straightforward. Any adjustment made to one parameter can have an undesired effect on another. Also, for many processes that are modeled, relevant observational data is difficult to acquire, and thus it is hard to know which parameters are behaving improperly.
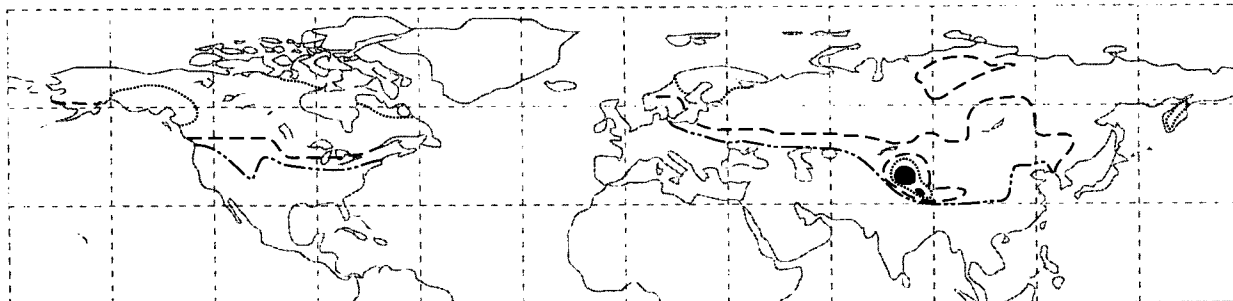
ECHAM Mean February Snow Depth
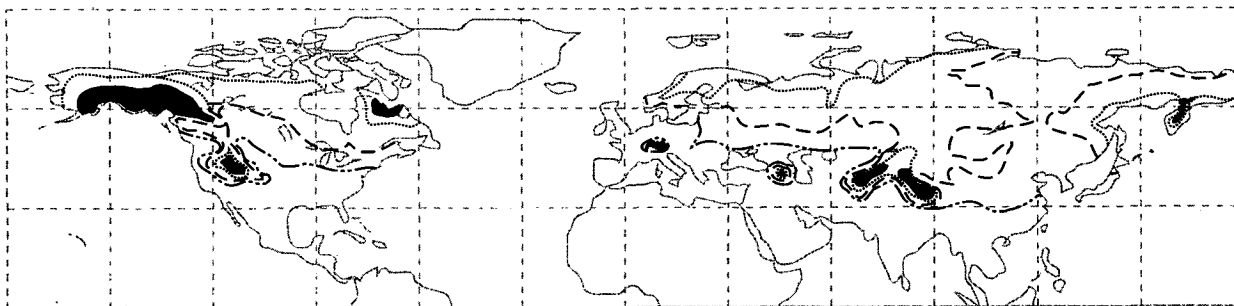
Contour at 2, 25, 50 and 75 cm snow depth

FIG. 16. Same as Fig. 10 except from the ECHAM GCM.

GENESIS Mean February Snow Depth

Contour at 2, 25, 50 and 75 cm snow depth

FIG. 17. Same as Fig. 10 except from the GENESIS GCM.

It should be noted that it is not always those models that seem to mimic the snow cover or snow mass most accurately that have the most realistic parameterizations. On a continental basis, it may appear that the snowpack is modeled correctly, but a number of parameters may be misrepresented in such a way that the modeled results are close to what is observed. For instance, the level of eddy activity may be systematically underestimated, but snowfall may be overestimated if temperatures are too cold (Behr and Dumenil 1992). The answer to where problems exist geographically and what the magnitude of the errors are have been presented in the previous section. Now that the where and the what have been better defined we can discuss the question as to why there are differences.

a. ECHAM model

With the ECHAM model, the main discrepancy is the excess of snow that occurs during the melt season (April and May). There may be several reasons why this occurs, including the favored production of snowfall instead of rainfall, improper melting processes, the specification of snow albedo, or the fact that this model does not allow for the influence of rain on snow, which can provide large amounts of energy for melting (Behr and Dumenil 1992). However, since relevant data at required scales is often difficult to collect, it is hard to know which of these various processes may be the source of error.

Temperature errors alone in the model do not seem to explain the excess of snow in the spring. Temperatures are too cold in the spring in the vicinity of the snowline with the ECHAM model, and this favors snowfall over rainfall, so there is an excess of snow mass at this time of year. Concerning precipitation, it appears that north of 50° in North America, at least, the model produces more precipitation than the observed climatology. The strength and paths of midlatitude cyclones seems to be represented fairly well, even though

too much snowfall is produced at the level of cyclone activity in the ECHAM model. A scenario that may be happening with this model is that snow is melting in the model at a rate similar to that of the observed melt, but the melting is not expeditious enough to counterbalance the heavy snowfalls produced in the model in March and April. The parameterization of the physical processes concerned with condensation in this model needs to be further examined.

b. HC model

With the HC model, there is a large excess of snow mass produced in the summer and fall in North America despite the fact that the modeled snow extent values are very close to what is observed. In some high-altitude, high-latitude grids, the snowpack is continuing to increase to the degree that snow accumulation is overwhelming snowmelt. About 70% of the excess mass is concentrated at one grid point in the Alaska ranges of southeastern Alaska. This excess snow load carries over into the fall, since it takes time for the modeled snowpack to reach equilibrium. In Eurasia, the excess in summer and fall snow mass is not as much of a problem.

Reducing the diffusion applied to the atmospheric model fields has been found to produce more realistic precipitation over steep orography, but the Alaskan anomaly was already present in the snow depth field used to initialize the model, which was obtained from a previous model integration. The impact of using a more realistic initialized snow field to determine its consequences on snow mass in the summer is being explored.

c. GLA model

A dominant feature of the GLA GCM simulation is the relatively high snow mass values computed for April and May in both North America and Eurasia. This

GISS Mean February Snow Depth
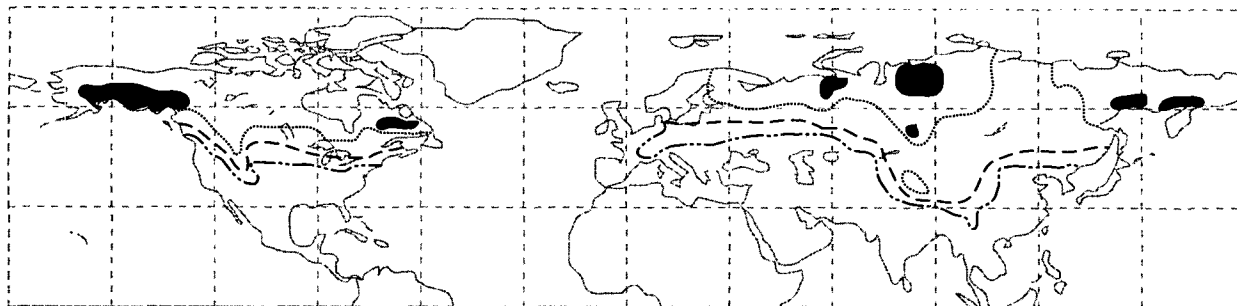
Contour at 2, 25, 50 and 75 cm snow depth

FIG. 18. Same as Fig. 10 except from the GISS GCM.

occurs despite the simulation of apparently realistic snow cover extent during all seasons of the year. A comparison between the USAF snow depth climatology and the GLA monthly mean snow mass shows that the shape and magnitude of the seasonal evolution of snow mass is quite well represented, but that the phase of the modeled distribution curve is shifted by one month. This results in a North America snow mass peak in March and April, when the snow depth climatology indicates that it should fall during February and March. In addition, the snow mass simulated during the fall and winter months is lower than that indicated by the observed climatology.

This lack of realism in the snow mass simulation during the spring months highlights the often-noted difficulty in obtaining precise climate model simulations during the transition months between the summer and winter seasons. In this case the snow mass is strongly dependent upon the simulated surface-energy balance, its associated surface-air temperature, and the precipitation field, all of which are coupled to the model hydrodynamics and other physics parameterizations.

A comparison of model-produced and observed (Schemm et al. 1992) surface-air temperature and precipitation fields indicates that the model-produced precipitation in North America is roughly 55% higher than the observed precipitation during the months of March, April, and May. During these same months, the modeled surface air temperatures are nearly identical to the observations. In contrast, though, the modeled air temperatures from October through February are higher, by roughly 2°C. These higher temperatures inhibit the accumulation of snow, despite the overproduction of precipitation by the model, and lead to low snow mass during the fall and winter months. During the spring months, when temperatures are well simulated and still at or below freezing, the high precipitation produces a deep, late-season snowpack.

d. ARIES model

Figures 1, 3, 5, and 7 show several deficiencies in the snow budget generated by ARIES. Such deficiencies are not surprising, given that little attention had been paid to the model's snow budget prior to this study. ARIES, a relatively new GCM, has primarily been used for studies of land/atmosphere interaction, which are strongest during summer, and for tropical ENSO studies.

During summer, at least, the seemingly overestimated snow cover and snow mass over North America are artifacts of the diagnostic procedure and do not reflect a true model error. The model does not really have that much summer snow.

The other deficiencies in the snow budget, namely, the underestimation of snow mass during winter and the delayed melting of snow during spring, are real. To examine the extent to which these problems result from deficiencies in the GCM's temperature, precipitation, and sublimation fields, a simple algorithm was developed that converts time series of precipitation and temperature distributions into a time series of total snow mass. The algorithm works very well when applied to observations of temperature and precipitation; the resulting seasonal cycle of snow mass closely agrees with the SDC. By alternately applying observed and modeled fields into the algorithm, and by reducing modeled precipitation by modeled sublimation in some applications, the analysis shows that (a) snowfall is not greatly underestimated during fall and winter in the GCM, (b) sublimation in the model appears to be excessive, and (c) modeled temperatures appear to be too cold in spring, delaying snowmelt.

This method of examining snowpack growth and decline is simplistic. However, it does point to likely causes of the model's snow deficiencies—excessive sublimation during winter and cold temperatures during spring. Excessive sublimation in the GCM is likely for two reasons: 1) in the current energy balance for-

mulation, all snow must evaporate before transpiration, bare soil evaporation, or interception loss can occur, and 2) the GCM's atmosphere is known to be excessively dry near the surface. An improved energy balance formulation that allows concurrent evaporation from snow and snow-free areas has already been devised and will be tested in the near future. The low springtime temperatures are probably related to the snow albedo formulation. The snow albedos used for visible and near-infrared radiation are constant regardless of snow age or whether the snow is wet and melting. Thus, they are probably too high during spring, leading to low values of absorbed solar radiation. Changes in the snow albedo formulation will be introduced, which should bring the model's spring temperatures closer to the observed.

e. GENESIS model

With the GENESIS model, the spring snow cover falls off too soon, and in the fall, it increases too late. Conversely, snow mass is equal to or greater than the SDC values in these transition periods (and in winter as well).

In this model there is a minimum snow column thickness of 15 cm. As a previously snow-free grid box starts to accumulate snow, the fractional cover increases from zero with the snow-column depth fixed at 15 cm. Only after the fractional cover reaches 1.0 can the column thickness increase. The reverse sequence occurs when snow goes away. Since the spring/fall snow cover is too low but the total mass is realistic, this suggests that the arbitrary minimum thickness of 15 cm is too large. If this value was changed to 5 cm for instance, the fractional cover in partially covered grid boxes would be larger for the same amount of snow mass.

This model attempts to predict sea ice and SSTs, so the surface-air temperature errors are generally somewhat larger than in those AMIP models, which use prescribed SSTs. Since the distinction between rainfall and snowfall is determined simply by whether the surface-air temperature is above or below freezing, temperature errors in midlatitudes could lead directly to errors in the movement of the snow cover boundary in spring and fall.

f. GISS model

The GISS model produces deficient snow mass almost every month of the year. The only months in which the GISS model produces excessive snow mass are the warmer months. During the Northern Hemisphere's winter, model temperatures are too warm, especially at midlatitudes. Warmer-than-observed temperatures would decrease the extent and thickness of the snow at mid-to-high latitudes, when compared with observations, producing deficient snow cover and snow mass. On the other hand, model temperatures are too

cold during the Northern Hemisphere's summer at high latitudes. During the warm months, colder-than-observed temperatures decrease snow melt, resulting in excessive snow depths. Therefore, the change in error from winter to summer temperatures produces deficient snow mass in winter and excessive snow mass in summer.

Another contribution to deficient snowfall in the GISS model is the stratiform precipitation patterns from extratropical cyclones. It was found that storms have deficient precipitation on the west or cold side of the storm track. Because much of a storm's snow occurs to the west of the storm track, this model error would directly lower snow cover and snow mass during the snow growth season.

g. CCC model

From the monthly modeled and observed snow extent and snow mass data for North America, it can be seen that version II of the CCC GCM reproduces observed values fairly closely. There is a slight tendency toward winter overestimation of both variables; as demonstrated by the February data. This is largely caused by a tendency in the model to deposit snow too far south along the Rockies. This may be caused by the relatively coarse resolution of the model, which leads to smoothing of mountainous topography, which could, in turn, be causing moisture from the Pacific to be deposited too far inland. Tests using a regional version of the GCM have shown that this problem disappears at high resolutions. The overestimation of snow mass in the American Rocky Mountain basin is counterbalanced by an underestimation of snow accumulation in Quebec and Labrador; the latter seems to be caused by insufficient moisture convergence from the Atlantic over the region, which is possibly related to the strong winter circumpolar westerlies simulated by the model.

Without a comparable AMIP run carried out using the CCC GCM's second-generation, land-surface model CLASS (Verseghy 1991), it is hard to say what aspects of the simulation are caused by the crudeness of the land-surface model used in this run. However, more recent evidence (Verseghy 1992) shows that the latter model tends to produce delays in snow accumulation and freezing of the soil in winter, and similar delays in snow melting and soil thawing in the spring. This effect indeed can be seen in the snow extent and snow mass data for both North America and Eurasia; it will be instructive in the future to compare these results with an AMIP run using the next generation of the GCM, which is planned to have CLASS incorporated as the operational land-surface model.

Turning to the results obtained for Eurasia, it can be seen that the CCC GCM overestimates both snow extent and snow mass in the winter and spring by a considerable amount. Looking at the February maps for the model and for observations, it can clearly be seen

that the model actually does fairly well in all areas except for central Siberia and the Himalayas. (The Alps are too small an area to be well resolved at GCM scales.) In this region, what should be a large maximum of snow mass in central Siberia is actually split in two by the model, with part of this mass being deposited farther south in the Himalayas. The reasons for this behavior on the part of the GCM are currently under investigation, but seem to be related to a cold anomaly, which is persistently present yearround over the Himalayan area and which may be causing westerly storm tracks to veer too far south, at least during the winter.

h. SMMR data

Comparisons with NOAA data of snow cover percentage differences, show that the SMMR microwave data are in closer accord with the Eurasian snow measurements than with the North American measurements. A partial explanation for this is the difference in size between these two landmasses. Eurasia is more than double the size of North America, and its snow cover at the time of maximum extent in January and February is about twice as large. Looking at Fig. 1, the absolute snow cover difference between the SMMR and the NOAA measurements for North America in February is about 1.1×10^6 km^2. For Eurasia (Fig. 5) the absolute difference is about 0.4×10^6 km^2. However, the percentage difference is 7.4% and 1.4% for North America and Eurasia, respectively.

The microwave snow cover area for North America is less than the estimates from the NOAA data for every month. This may be attributable to the ineffectiveness of microwave radiation in providing information about shallow snow cover as mentioned below. Because North America has a larger portion of its surface area located at lower latitudes than does Eurasia, it is reasonable that a larger portion of its snow cover is transitional and ephemeral in nature. This may help to account for the differences in snow extent between NOAA and the microwave data for Eurasia and North America.

As with snow extent, with snow mass there is typically closer agreement in Eurasia than in North America between the climatological data and the microwave data, in terms of percentage difference. For example, for North America in December, the percentage difference between SMMR and the climatological data is about 59%. For Eurasia, the percentage difference is about 23%. The absolute difference is 68×10^{13} kg and 56×10^{13} kg for North America and Eurasia, respectively.

With the SMMR data, the most prominent error feature is the underestimation of snow mass during the winter, especially for North America. Snow cover values are only slightly lower in winter than the NOAA snow extent measurements. When the band of snow near the southern limit of the continental snowline is

sufficiently shallow (<3 cm), then the radiation welling up from the ground may pass through the snowpack virtually unimpeded (Foster et al. 1993). Therefore, in the vicinity of the snowline, the snow mass also will be smaller than observed. During the winter months, probably less than 5% of the total snow-covered area is too shallow to be detected using the passive microwave data.

The most likely reason why the microwave data underestimates snow mass has to do with the effects of vegetation above snow fields. With the microwave data, the emissivity of trees, especially dense conifers, can overwhelm the scattering signal that results when microwave energy is redistributed by snow crystals.

The boreal forest zone, which stretches across the northern tier of North America and Eurasia, is perhaps the physiographic region where most of the difference occurs between the snow depth measurements based on climatological data and those based on microwave observations. Forests not only absorb some of the radiation scattered by snow crystals, but trees are also emitters of microwave radiation. So in forested areas, the signal received by a radiometer onboard a satellite is produced by a combination of media. Generally, the denser the forest, the higher the microwave brightness temperature, despite the type and condition of the media underlying the forest canopy. Furthermore, because the canopy shields the snow from direct solar radiation, the deepest snows accumulate in the densest forests (Foster et al. 1995).

However, if the fractional forest cover of a given microwave pixel can be accounted for in some way, then microwave algorithms can be modified by including a forest cover parameter, and estimates of snow depth will be improved. A normalized vegetation index, derived from global reflectance data, has been used as an indicator of forest cover, and preliminary results show that a refined algorithm that incorporates this index compares more favorably with climatological snow depths.

Additionally, efforts are ongoing to use adjusted values for snow grain size, which can vary from one physiographic or climatic region to another. The Chang et al. (1987) algorithm assumes an average grain size of 0.3 mm for the entire snowpack, regardless of geographic location. More realistic snow mass values may be attained if snow grain sizes are based on field observations for a specific region such as the boreal forests.

6. Conclusions and future directions

This intercomparison study has shown where discrepancies exist and what the magnitude of the discrepancies are between the observed snow data and results from several GCMs and from passive microwave satellite data. In general, the GCMs simulate snow cover conditions reliably in most months, except in Oc-

tober, when snow begins to expand southward. In terms of snow mass, the models perform better during the winter months than during the transitional spring and autumn months. There is a lack of realism in simulating the snow mass at these times primarily because of inaccuracies in modeling precipitation and temperature fields in the early fall and late winter.

Concerning the passive microwave results, snow cover values from the SMMR sensor compare favorably with the NOAA values for most months. However, it has been shown that a derived algorithm, which uses only a single coefficient and the difference between the 18-GHz and 37-GHz channels to estimate snow mass, is neither very reliable nor accurate. For example, when compared to the climatological data for North America, the Chang et al. (1987) algorithm underestimates snow mass by more than 50% from December through March.

A primary reason to study, evaluate, and quantify the GCMs is to assess how reliably they can predict future climate change. Climate models have predicted $2°-5°C$ warming in a doubled CO_2 climate. However, most of the warming is thought to occur at high latitudes because of the positive feedback of melting snow cover and sea ice. How global snow cover and land ice will react to warmer global temperatures is presently a controversial issue. Currently, various GCMs have very different snow climate feedbacks. Some have strongly positive feedbacks and others have weakly negative feedbacks (Cess et al. 1991). The modeling community needs to make significant improvements in order to gauge correctly the interactions of a warming climate and snow cover (Cohen 1994).

Understanding the capabilities and limitations of GCMs is important also for sensitivity studies of hydrologic models and for programs such as the Global Energy and Water Cycle Experiment (GEWEX), which is concerned with hydrologic and energy cycles and their complex interactions between the land surface and the atmosphere. In addition, how a particular snowmelt model incorporates results from GCMs is essential to forecasting runoff and assessing future water supply.

In essence, this work is the first attempt to look at continental differences in snow conditions using several datasets. Although new information has been acquired concerning the temporal and spatial variations that exist among the datasets, more work needs to be done to learn if snow buildup and snowmelt processes are being adequately handled by the models and the microwave datasets in specific physiographic or climatic provinces. For instance, by looking at microwave snow data and model output in the boreal forest region, a determination can be made as to whether the models and the microwave algorithms perform differently here than for the continent as a whole. Perhaps some of the GCMs model snow conditions accurately for continental scales, but on a regional basis the accuracy is much poorer. This needs to be documented, and then the

question as to why this may be the case can be addressed.

REFERENCES

Arpe, K., H. Behr, and L. Dumenil, 1993: Validation of the ECHAM models with respect of precipitation, snow and river runoff: Analysis methods of precipitation on a global scale. Report of a GEWEX workshop, WCRP-81, WMO-TD-No. 558, A/104–A/122.

Barnett, T. P., L. Dumenil, U. Schlese, and E. Roeckner, 1987: The effect of Eurasian snow cover on global climate. *Science,* **239,** 504–507.

Behr, H., and L. Dumenil, 1992: The snow climatology in decadal model simulations. Studying climate with the atmospheric model ECHAM. Report No. 9, R. Sausen, Ed., Meteoroligisches Institut der Universität Hamburg, 53–81.

Briegleb, B., and V. Ramanathan, 1982: Spectral and diurnal variations in clear sky planetary albedo. *J. Appl. Meteor,* **21,** 1160–1171.

Cattle, H., 1991: Global climate models and Antarctic climate change. *Antarctic and Global Climate Change,* G. M. Harris and B. Stonehouse, Eds., Belhaven Press, 21–34.

Cess, R. D., and Coauthors, 1991: Interpretation of snow-climate feedbacks as produced by 17 general circulation models. *Science,* **253,** 888–892.

Chang, A. T. C., J. L. Foster, and D. K. Hall, 1987: *Nimbus-7* SMMR derived global snow cover parameters. *Ann. Glaciol.,* **9,** 39–44.

Cohen, J., 1994: Snow cover and climate. *Weather,* **49,** 150–155.

Dickinson, R. E., A. Henderson-Sellers, P. J. Kennedy, and M. F. Wilson, 1986: Biosphere–Atmosphere Transfer Scheme (BATS) for the NCAR Community Climate Model. National Center for Atmospheric Research, Boulder, CO, NCAR/TN-275+STR, 69 pp.

Fischer, G., 1987: Climate simulations with the ECMWF T21-model in Hamburg. Large Scale Atmospheric Modelling, Report No. 1, Meteorologisches Institut der Universität Hamburg, Hamburg, Germany.

Foster, D. J., Jr., and R. D. Davy, 1988: Global snow depth climatology. USAF publication USAFETAC/TN-88/006, Scott Air Force Base, Illinois, 48 pp.

Foster, J. L., G. Liston, R. Essery, H. Behr, L. Dumenil, D. Verseghy, R. Koster, S. Thompson, D. Pollard, and J. Cohen, 1994: Intercomparison of snow cover and snow mass in North America from general circulation models and remote sensing. *Proc. Sixth Conf. on Climate Variations,* Nashville, TN, Amer. Meteor. Soc., 207–211.

——, A. T. C. Chang, R. J. Gurney, F. Hewer, and R. Essery, 1995: Snow cover and snow mass estimates from remote sensing, climatology and the United Kingdom Meteorological Office general circulation model. *Proc. ESA/NASA Passive Microwave Workshop,* St. Lary, France, in press.

Geleyn, J. F., and H. J. PreuB, 1983: A new data set of satellite derived surface albedo values for operational use at ECMWF. *Archiv. Meteor. Geophys. Bioklimatol.,* Series A, **32,** 353–359.

Gregory, D., and R. N. B. Smith, 1990: Canopy, surface and soil hydrology. Unified Model Documentation, Paper 25, UKMO, Bracknell, United Kingdom, 19 pp.

Groisman, P. Y., R. C. Quayle, and D. R. Easterling, 1993: The need for correction of systematic errors in conventional precipitation climatologies. GEWEX News, Vol. 3, No. 2, 8–11.

Hansen, J., G. Russell, D. Rind, P. Stone, A. Lacis, S. Lebedeff, and L. Travis, 1983: Efficient three-dimensional global models for climate studies: Models I and II. *Mon. Wea. Rev.,* **111,** 609–662.

Harvey, L. D. D., 1988: Development of a sea ice model for use in zonally averaged energy balance climate models. *J. Climate,* **1,** 1221–1238.

Koster, R., and M. Suarez, 1992: Modeling the land surface boundary in climate models as a composite of independent vegetation stands. *J. Geophys. Res.,* **97,** 2697–2715.

——, and ——, 1994: The components of a SVAT scheme and their effects on a GCM's hydrological cycle. *Adv. Water Resour.,* **17,** 61–78.

Longley, R. W., 1960: Snow depth and snow density at Resolute, Northwest Territories. *J. Glaciol.,* **3,** 733–738.

Matson, M., and D. Wiesnet, 1981: New data base for climate studies. *Nature,* **289,** 451–456.

——, C. Ropelewski, and M. Varnadore, 1986: An atlas of satellite derived Northern Hemisphere snow cover frequency. Department of Commerce, Washington, D.C., 75 pp.

Matthews, E., 1983: Global vegetation and land use: New high-resolution data bases for climate studies. *J. Climate Appl. Meteor.,* **22,** 474–487.

Robock, A., 1980: The seasonal cycle of snow cover, sea ice and surface albedo. *Mon. Wea. Rev.,* **108,** 267–285.

Roeckner, E., and Coauthors, 1992: Simulation of the present-day climate with the ECHAM model: Impact of model physics and resolution. Max-Planck-Institut für Meteorologie, Report No. 93, Hamburg, Germany.

Schemm, J., S. Schubert, J. Terry, and S. Bloom, 1992: Estimates of monthly mean soil moisture for 1979–1989. NASA Tech. Memo. 104571, National Aeronautics and Space Administration, Greenbelt, MD, 260 pp.

Sellers, P. J., Y. Mintz, Y. C. Sud, and A. Dalcher, 1986: A simple biosphere model (SiB) for use within general circulation models. *J. Atmos. Sci.,* **43,** 505–531.

Smith, R. N. B., 1993: Subsurface, surface and boundary layer processes. Unified Model Documentation, Paper 24, UKMO, Bracknell, United Kingdom, 75 pp.

Thompson, S. L., and D. Pollard, 1994: A global climate model (GENESIS) with a land-surface transfer scheme (LSX). Part 1: Present climate simulation. *J. Climate,* **7,** 732–761.

Verseghy, D. L., 1991: CLASS-A Canadian land surface scheme for GCMs. Part 1: Soil moisture. *Int. J. Climatol.,* **11,** 111–133.

——, 1992: Snow modelling in general circulation models. Snow Watch '92 Proc. Glaciological Data Report GD-25, R. G. Barry, B. E. Goodison, and E. F. LeDrew, Eds., Institute for Space and Terrestrial Science and the World Data Center A for Glaciology, 86–92.

Walsh, J. E., and B. Ross, 1988: Sensitivity of 30 day dynamical forecasts to continental snow cover. *J. Climate,* **1,** 739–754.

Xue, Y., P. J. Sellers, J. L. Kinter, and J. Shukla, 1991: A simplified biosphere model for global climate studies. *J. Climate,* **4,** 345–364.